

Chapter 1

Non-parametric Mixture Model Based Evolution of Level Sets

Niranjan Joshi and Michael Brady
*Wolfson Medical Vision Laboratory,
University of Oxford,
Parks Road, Oxford OX1 3PJ, UK.
njoshi@robots.ox.ac.uk*

We present a novel region-based level set algorithm. We first model the image histogram with a mixture of non-parametric probability density functions (PDFs), whose use we justify. The individual densities in the mixture are estimated using a recently proposed PDF estimation method which relies on a continuous representation of discrete signals. A Bayesian framework is then formulated in which likelihood probabilities are given by the non-parametric PDFs and prior probabilities are calculated using an inequality constrained least squares method. The segmentation solution is spatially regularised using a level sets framework. The log ratio of the posterior probabilities is used to drive the level set evolution. We also take into account the partial volume effect, which is important in medical image analysis. Results are presented on natural, as well as medical, two-dimensional images. Visual inspection of results on a range of images show the effectiveness of the proposed algorithm.

1.1 Introduction

Segmentation is a fundamental image analysis technique and has found application in many fields, ranging from satellite imagery to medical imaging. Design of a typical image segmentation method involves modelling of the data and spatial regularisation of the segmentation solution. Here, we present a method in which we model the histogram of image intensities using a mixture model and regu-

larise the segmentation solution using level set methods. Although the method presented in the rest of this paper is sufficiently general to be applied to any kind of image, indeed we provide such an example, we are mainly interested in medical applications, particularly colorectal cancer image analysis.

Finite mixture model(FMM) methods are widely used in image segmentation. They assume that the image is comprised of a finite number of classes and that the intensities of each class follow a certain distribution. Gaussian mixture models(GMMs) are a popular instance of FMM methods[Zhu and Yuille (1996); Paragios (2000)]. They have the advantage of simplifying analytical treatment of the problem. While the assumption of class Gaussianity works well in many situations, a more generalised approach is to use non-parametric probability density/mass functions (PDFs/PMFs) to model the individual classes. We adopt the latter approach for the reasons discussed in Sec. 1.2. We refer to our mixture model as a non-parametric mixture model(NPMM)[Joshi and Brady (2005); Joshi (2005)]. Several methods are available to estimate the class non-parametric distributions, such as: histograms and kernel density estimates[Izenman (1991)]. However, histograms need a large number of samples to give smooth estimates and the kernel density estimates need proper selection of the bandwidth parameter of the kernel. The NP-window method[Kadir and Brady (2005); Joshi (2005)] used here attempts to overcome both these drawbacks. This method is briefly explained in Sec. 1.3.

Level set methods have been used successfully for curve evolution. Typically, these curves coincide with the boundaries of the segmentation classes. Because of the implicit nature of level set curve evolution, they can accommodate changes in topology of the curve, for example, across successive slices of a medical image volume. Available level set methods can be broadly divided into three categories: boundary-based methods[Caselles *et al.* (1997)], region-based methods[Zhu and Yuille (1996); Kim *et al.* (2005)], and combination of both[Paragios (2000)]. In our method, we use region-based forces to evolve the level sets. The region based forces are calculated using knowledge of the NPMM of the image. Brief introduction to level set terminology and how we use them in our segmentation method are given in Secs. 1.5 and 1.6 respectively.

As we mentioned earlier, our work is motivated by application to medical images. Therefore, we also consider certain issues that are particularly important to this field, for instance, the partial volume effect (PVE). Due to the limited resolution of a medical image acquisition system, any single pixel/voxel in the image may contain more than one kind of physical tissues[Leemput *et al.* (2003); Joshi (2005)]. As a result the intensity value at this pixel is a linear (or non-linear) function of the individual tissue intensities depending upon the acquisition

modality. In certain medical images as many as 40% of the total pixels may be affected by the PVE. Hence it is important to take this effect into account while designing any of the analysis methods for such images. In Secs. 1.4 and 1.6, we describe how we take the PVE into account.

1.2 Need for Modelling Class Distributions Non-parametrically

Most of the statistical mixture model methods in the current medical image analysis literature assume Gaussianity for individual class PDFs. This leads to straightforward analytical treatment of the problem. While, theoretically, the noise distribution in a magnetic resonance (MR) image is a Rician distribution, towards high signal to noise ratio (SNR) this tends to be a Gaussian distribution [Sijbers (1998)]. A few methods are also reported to have performed special transformation of intensity values in order to increase the Gaussianity of the data, where the individual class PDFs do not follow Gaussian distribution [Zeydabadi *et al.* (2004)]. This is how generally the use of the Gaussian distribution assumption is justified in MR image segmentation. This holds better for brain MR images where field coil technology is sufficiently advanced to give better quality images and the images are intrinsically more or less piecewise smooth. However such assumptions may not hold true for MR images of the other body parts, e.g. the colorectum, in which we are particularly interested. Due to magnetic field inhomogeneities in the MR scanner, some parts of the image appear 'brighter' or 'darker' than other parts. This is referred to as the bias field distortion. The bias field distortion due to body coils in the case of colorectal MR images is of such magnitude that a significant residue remains even after applying available preprocessing methods. The segmentation of colorectal MR images involves dividing the image into the colorectum, tumour, and mesorectum. While the tumour tend to be a heterogeneous mass, the mesorectum is chiefly made up of layers of fat, blood vessels, and lymph nodes. Due to these anatomical properties the colorectal MR image is not piecewise smooth. See Fig. 1.1 for a visual illustration. As a result, the shapes of the distributions of the individual classes are distorted, usually in a way that is unpredictable. Figure 1.2 shows one such example of the class PDFs. Primarily, to take all these effects into account we model the class PDFs using non-parametric distributions. However at the same time the use of non-parametric distributions has the potential of making the segmentation method more generally applicable and this is further illustrated in Sec. 6.5.

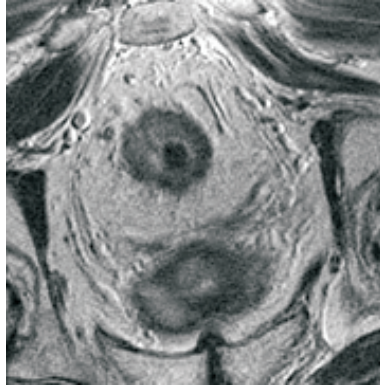


Fig. 1.1 One slice of a 3-dimensional (3D) colorectal MR image after preprocessing done to remove bias field. Notice the residual bias field in the upper part of the image and a complex heterogeneous nature of the central part of the image.

1.3 NP-windows Method for Non-parametric Estimation of PDFs

Recently Kadir and Brady proposed [Kadir and Brady (2005)], and we further developed [Joshi (2005)], a method to estimate the PDF of a discrete signal using a continuous representation. The method is based on the observation that a critically sampled or oversampled discrete signal can be reconstructed to the original continuous signal if an appropriate interpolation procedure is employed. Additional information, modelled in the interpolation method, helps to improve PDF estimation. For reasons of space, we limit the discussion here to 2-dimensional (2D) signals and to bilinear interpolation, though neither of these restrictions are intrinsic to the method.

Consider a 2-dimensional (2D) image. Let Y_1 denotes the intensity variable (in this section, all variables will be denoted by upper case letters and their particular values will be denoted by lower case letters). Continuous random variables X_1 and X_2 denote positional variables in 2D. We divide the image into several piecewise sections. The intensity variable Y_1 is deterministically related to the positional variables over these piecewise sections. Typically this relationship is polynomial. Our objective is to find out the PDF of the intensity values, given the nature of randomness in the positional variables and the deterministic relationship. In this paper it is assumed that Y_1 is related to the positional variables by bilinear interpolation over a piecewise section by joining the centres of four neighbouring pixels. This case was originally proposed in [Kadir and Brady (2005)]. Next, it is assumed that the positional variables are uniformly distributed over this piecewise

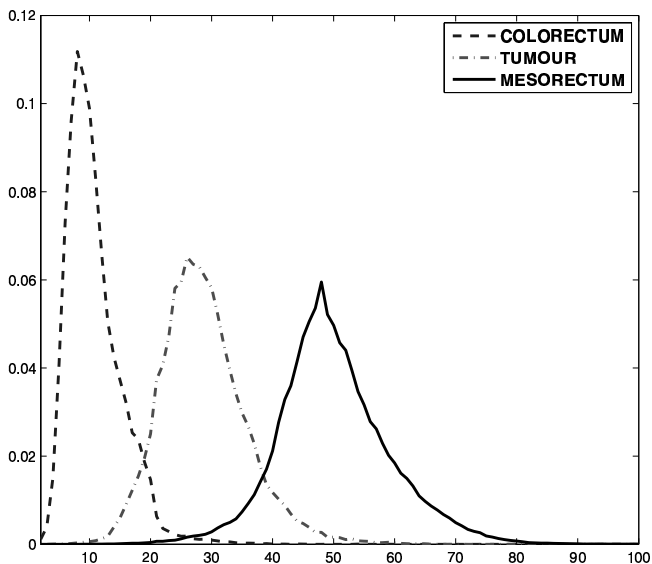


Fig. 1.2 Histograms of three different tissue classes in a 3D colorectal MR image. Notice the asymmetric nature of the probability distributions. This is mainly because of the residual artifacts such as bias field that remain after preprocessing, and also due to nonconformity to piecewise smooth image assumption.

bilinear region i.e. $f_{X_1, X_2}(x_1, x_2) = 1$ for $0 \leq x_1, x_2 \leq 1$, where $f(\cdot)$ denotes a PDF. Hence the following equations, in which Y_2 is a dummy variable, can be written:

$$y_1(x_1, x_2) = ax_1x_2 + bx_1 + cx_2 + d, \quad y_2(x_1, x_2) = x_1 \tag{1.1}$$

$$x_2(y_1, y_2) = \frac{y_1 - by_2 - d}{ay_2 + c}, \quad x_1(y_1, y_2) = y_2 \tag{1.2}$$

The joint PDF f_{Y_1, Y_2} can be calculated by using the transformation formula for functions of random variables [Papoulis and Pillai (2002)]. In particular,

$$f_{Y_1, Y_2}(y_1, y_2) = f_{X_1, X_2}\left(y_2, \frac{y_1 - by_2 - d}{ay_2 + c}\right) |J| \tag{1.3}$$

where, $|J|$ is the Jacobian and is equal to $|1/(ay_2 + c)|$ in this case. Therefore,

$$f_{Y_1, Y_2}(y_1, y_2) = \frac{1}{ay_2 + c} \tag{1.4}$$

subject to,

$$0 \leq y_2 \leq 1 \quad \text{and} \quad 0 \leq \frac{y_1 - by_2 - d}{ay_2 + c} \leq 1 \tag{1.5}$$

The marginal PDF f_{Y_1} is obtained by integrating out the dummy variable Y_2 over the ranges given in Eq. (1.5). The ranges of integration are shown graphically in Fig. 1.3. Note that the specific geometry of a configuration is determined by values

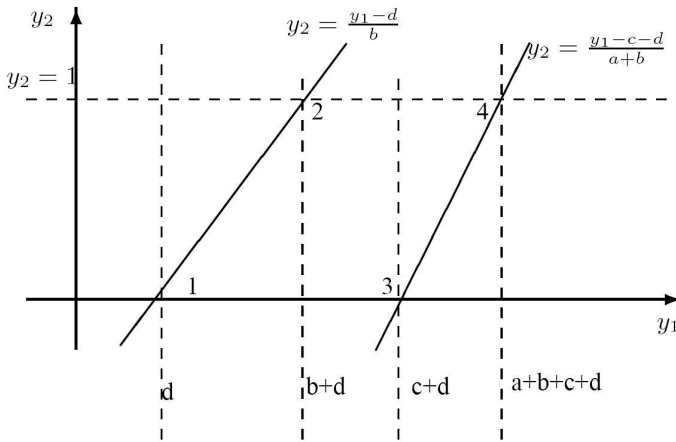


Fig. 1.3 Shown here is the particular configuration for $\{b, c, d\} > 0$, $a < 0$ and $a + b > 0$, which results into three different integration ranges marked by dashed lines.

of the coefficients in Eq. (1.1). In their original proposition [Kadir and Brady (2005)], the authors point out that there are 24 such configurations are possible, corresponding to $4!$ ways of arranging the values of the four corner pixels of the piecewise bilinear section. We have reduced the number of configurations in our implementation, which makes it simpler and faster than the original one. However due to space limitations we omit all the details related with implementation. The PDF obtained over each piecewise bilinear section is added and normalised to get the PDF of the given image.

A few comments are in order before we proceed further to look into applications of the NP windows method. The NP windows method converts the given discrete signal to its continuous counterpart based on the chosen interpolation method. Therefore the PDF estimate thus obtained is also the continuous one. In most applications in image processing we need the PMF of the discrete intensity values and this can be obtained by binning the PDF estimate. The bin width is dependent on the application and in most cases can be set naturally. The NP window estimate tends to be much smoother than the histogram estimate even for a small number of samples. This is because the NP windows estimate takes into account

the information not only at the discrete locations but also the information at the in between locations. Such interpolated information is appropriate as long as the signals are smooth enough or in other words band limited. Comparing with the kernel estimators, we notice that in the case of the NP windows method there is absolutely no need to set up any parameters at all once we assume an interpolation model. The NP windows method is data driven, which can be seen from the fact that the coefficients in Eqs. 1.4 and 1.5 are all calculated from the input samples. Thus for smooth signals the NP windows method overcomes the drawbacks of both the histogram and the kernel estimators. Figure 1.4 shows various estimates of PMF for the given test image. The above statements can be visually assessed by looking at the estimates.

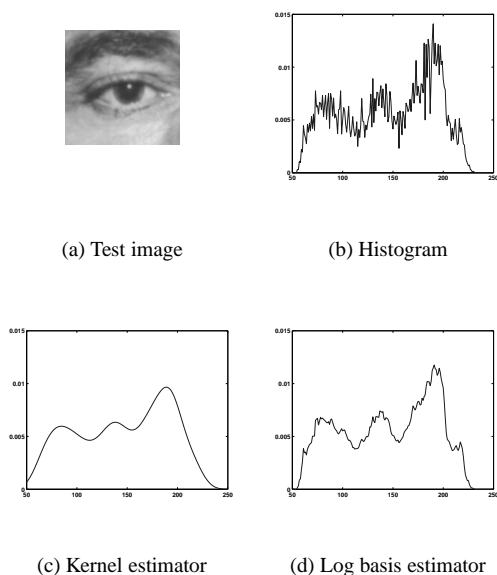


Fig. 1.4 Graphical plots of the various PMF estimates. While the histogram estimate appears very spiky, the kernel estimate tends to be oversmooth for a given kernel bandwidth setting. The NP windows estimate provides a balance between the two.

1.4 NPMM-ICLS Framework

We have presented a detailed account of this method in [Joshi (2005); Joshi and Brady (2005)]. Let $\mathcal{S} = \{1, 2, \dots, S\}$ be the set of indices for pixels of the image under consideration, where S is the number of pixels in the image. Let $Y = \{Y_1, Y_2, \dots, Y_S\}$ be the observed intensity image, and y_i be a particular

instance of the random variable Y_i . $y_i \in \mathcal{I} = \{0, 1, \dots, I_{max}\}$, where I_{max} depends upon the number of possible intensity levels in the image; for example in an 8-bit grey scale image $I_{max} = 255$. Let $X = \{X_1, X_2, \dots, X_S\}$ be the underlying partial volume(PV) segmentation for the image and x_i be a particular instance of the random variable X_i ; such that $x_i \in \mathcal{L} = \{l_1, \dots, l_K, \dots, l_T\}$ where, \mathcal{L} is the set of all possible tissue class labels, K is the number of *pure* tissue classes, and T is the total number of tissue classes including *partial* tissue classes. Note that each l_j corresponds to a K -dimensional tuple $\mathbf{t}_j = [t_{j1} \dots t_{jK}]^T$ of the contributing tissue fractions of each pure tissue, such that $\sum_k t_{jk} = 1$.

The value of K is chosen after taking account of anatomical knowledge. To choose the value of T , we assume the image model mentioned in [Leemput *et al.* (2003)]. In their model, the observed intensity image is assumed to result from downsampling a high resolution image, with a downsampling factor M . The high resolution image is assumed to be free of PVE. With this assumption, the values that \mathbf{t}_j can take are fixed automatically. Figure 1.6 lists the tissue labels and corresponding tissue fractions for the case $K = 2$ and $M = 2$. Figure 1.5 further illustrates this concept. Let $\tilde{Y} = \{\tilde{Y}_1, \tilde{Y}_2, \dots, \tilde{Y}_q, \dots\}$ be the corresponding high

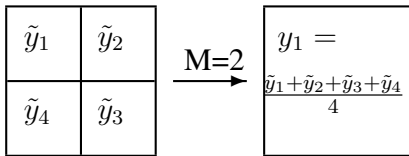


Fig. 1.5 Downsampling image model: (left) high resolution image, (right) low resolution image; here $M = 2$.

	t_{j1}	t_{j2}
l_1	1.00	0.00
l_2	0.00	1.00
l_3	0.25	0.75
l_4	0.50	0.50
l_5	0.75	0.25

Fig. 1.6 List of all tissue class labels and corresponding tissue fractions; $K = 2$ and $M = 2$.

resolution image and $\tilde{X} = \{\tilde{X}_1, \tilde{X}_2, \dots, \tilde{X}_q, \dots\}$ be the underlying segmentation. Note that \tilde{x}_q , a particular instance of the random variable \tilde{X}_q , is drawn from $\mathcal{L}' = \{l_1, \dots, l_K\}$, the set of only pure tissue class labels. We further assume that the random variables \tilde{Y}_q are conditionally independent, i.e.

$$P(\tilde{Y}|\tilde{X}) = \prod_q P(\tilde{Y}_q|\tilde{X}_q) \tag{1.6}$$

As shown in fig. 1.5, random variable Y_1 in the observed image is obtained by averaging four corresponding random variables $\tilde{Y}_1, \tilde{Y}_2, \tilde{Y}_3$, and \tilde{Y}_4 . Applying the conditional independence assumption and downsampling model for the image, it can be shown that the PMF

$$P(Y_1 = y_1|X_1 = x_1) = 4f(4y_1) \tag{1.7}$$

$$\text{where, } f(\cdot) = P(\tilde{Y}_1|\tilde{X}_1) * P(\tilde{Y}_2|\tilde{X}_2) * P(\tilde{Y}_3|\tilde{X}_3) * P(\tilde{Y}_4|\tilde{X}_4) \quad (1.8)$$

and * indicates convolution. Therefore, given an estimate of the PMFs for the pure tissue classes in the high resolution image, we can readily calculate the estimates of the basis PMFs of all tissues in the low resolution image.

In the following discussion, for notational convenience, we omit the suffices of the random variables Y_i s and X_i s. This should not lead to confusion because here we do not assume any spatial correlation, so the position of a pixel in the image does not affect the decision process of estimation of its class label. We now note that,

$$P(Y) = \sum P(Y|X)P(X) \quad (1.9)$$

where, $P(Y)$ is the overall intensity distribution, $P(Y|X)$ are the basis PMFs corresponding to each pure and partial class, and $P(X)$ is the prior PMF of all the classes. $P(Y)$ and $P(Y|X)$ are estimated using the NP-windows method described in the previous subsection. To estimate $P(X)$, we arrange the system of linear equations given in Eq.(1.9) in vector form: $\mathbf{p}_y = \mathbf{P}_{y,x} \mathbf{p}_x$ where, \mathbf{p}_y and \mathbf{p}_x are vectors, and $\mathbf{P}_{y,x}$ is a matrix whose columns represent the basis PMFs. In order to estimate \mathbf{p}_x , we seek a least squares solution of this equation. However we note that since \mathbf{p}_x represents a PMF; its elements must follow the positivity and summability constraints of a PMF. Hence we formulate the problem as follows:

$$\hat{\mathbf{p}}_x = \arg \min_{\mathbf{p}_x} \frac{1}{2} (\mathbf{P}_{y,x} \mathbf{p}_x - \mathbf{p}_y)^T (\mathbf{P}_{y,x} \mathbf{p}_x - \mathbf{p}_y)$$

subject to, $\mathbf{I} \mathbf{p}_x \geq \mathbf{0}$ and $\mathbf{u}^T \mathbf{p}_x = 1$ (1.10)

where, \mathbf{I} is the identity matrix, \mathbf{u} is a vector with all its elements equal to 1, and $\hat{\mathbf{p}}_x$ is the inequality constrained least square(ICLS) estimate of prior PMF of tissue classes. We adopt a Bayesian framework to obtain the following *maximum a posteriori* (MAP) estimate,

$$P(X|Y) = \frac{P(Y|X)P(X)}{P(Y)} \quad (1.11)$$

where, $P(X|Y)$ is posterior PMF of the pure and partial classes. The given pixel belongs to the class for which $P(X|Y)$ is maximum. We refer to this new algorithm as a non-parametric mixture model and inequality constrained least squares (NPMM-ICLS) algorithm.

1.5 Level Sets Method

Level set methods are used to evolve curves using partial differential equations. Consider a curve which is, for example, a boundary separating one image region

from another. It is assumed that the curve is moving along the normal direction at each point. The speed at which it moves depends upon local geometric properties such as the curvature κ at the point, as well as global properties such as integral of the image gradients along the curve. In order to accommodate arbitrary speed functions for evolution, instead of one curve a higher dimensional function ϕ is evolved. The function ϕ can be seen as a set of curves or levels, each of which evolves when ϕ evolves. The curve that interests us is typically chosen as $\phi = 0$ or the zero level set. In our case, we consider region-based level set methods. A typical level set evolution equation for this case can be written as follows,

$$\frac{\partial \phi}{\partial t} = [\kappa + \alpha F] |\nabla \phi|, \quad (1.12)$$

where the curvature $\kappa = \nabla \cdot (\nabla \phi / |\nabla \phi|)$, α is a constant, and F is a region based force term. The κ term provides geometric regularisation to the solution, whereas the region based term drives the solution towards a desired location in the image. So it now remains to choose this regional force term. That is the topic of discussion in the following subsection.

1.6 NPMM-ICLS Level Sets Method

Recall that our image model consists of a finite number of pure and partial classes. We presented earlier a NPMM based solution to segment an image. However our model did not consider any spatial regularisation and hence it was possible to get spatially disconnected solutions. We now propose to incorporate this NPMM-ICLS solution into the region-based level set framework. In particular, the curvature term will provide the spatial regularisation to our solution whereas NPMM will provide the regional force term. Suppose we have x_1, x_2, \dots, x_n pure classes. We consider n separate level set functions $\phi_1, \phi_2, \dots, \phi_n$, one for each pure class. For small n , it makes sense to use separate level sets functions for each class. We evolve each level sets function separately. So for each evolution equation we consider the following region based force.

$$F_{1n} = \log \left[\frac{P(Y|x_n)P(x_n)}{\sum_{i,i \neq n} P(Y|x_i)P(x_i)} \right] \quad (1.13)$$

Because the numerator of the $\log(\cdot)$ term denotes a *posteriori* probability, we refer to this term as \log a *posteriori* ratio force. The likelihood probabilities $P(Y|x_i)$ are the basis functions of our NPMM, and are estimated using the NP windows method described earlier. The mixture weights or the *a priori* probabilities are calculated using the NPMM-ICLS algorithm. While this regional force term could be

sufficient for many image analysis problems, in medical imaging applications we frequently need to take care of the PVE. We do this in the following manner. We formulate a second regional force term which inhibits the level sets to enter into the region which NPMM deems as a partial volume region. Let $f_{x_1}, f_{x_2}, \dots, f_{x_n}$ be the fractions of pure classes present in a pixel. Then the inhibition force term is given as,

$$F_{2n} = \sum_{i, i \neq n} f_{x_i} \quad (1.14)$$

Therefore the overall evolution equation of the n^{th} level set function is given as follows,

$$\frac{\partial \phi_n}{\partial t} = [\kappa + \alpha F_{1n} - \beta F_{2n}] |\nabla \phi_n| \quad (1.15)$$

We now summarise various steps of this new NPMM-ICLS level set formulation.

- (1) Initialisation: Draw initial curves manually. Calculate initial level set functions using the fast marching method. Calculate initial PMF estimates of pure and partial classes. Set initial mixture weights.
- (2) Estimate PMFs corresponding to pure classes using the NP windows method.
- (3) Calculate the log *a posteriori* ratio force.
- (4) Set the inhibition force term.
- (5) Evolve the the level set functions.
- (6) Calculate the mixture weights and partial volume fractions using NPMM-ICLS algorithm.
- (7) Repeat the steps (2) to (6) for a fixed number of iterations.

1.7 Results and Discussion

We have implemented this algorithm using a freely available level set method toolbox[Sumengen] in Matlab. We tested our algorithm on a set of medical images. The images used were colorectal magnetic resonance(MR) images. The image acquisition protocol comprised axial small field of view T2 weighted MR images (TE = 90ms, TR = 3500-5000ms, $\alpha = 90\text{deg}$, slice thickness = 3mm) acquired using a 1.5T MRI machine. We assumed three pure tissue classes namely, colorectum, tumour, and mesorectum. The original images contained whole abdominal section, which were then manually cropped to contain only region of interest.

Figure 1.7 shows the results of our new level set algorithm on four consecutive slices of a 3D colorectum MR image. We notice that all three solutions (corresponding to each level set function) are spatially continuous. This is due to the

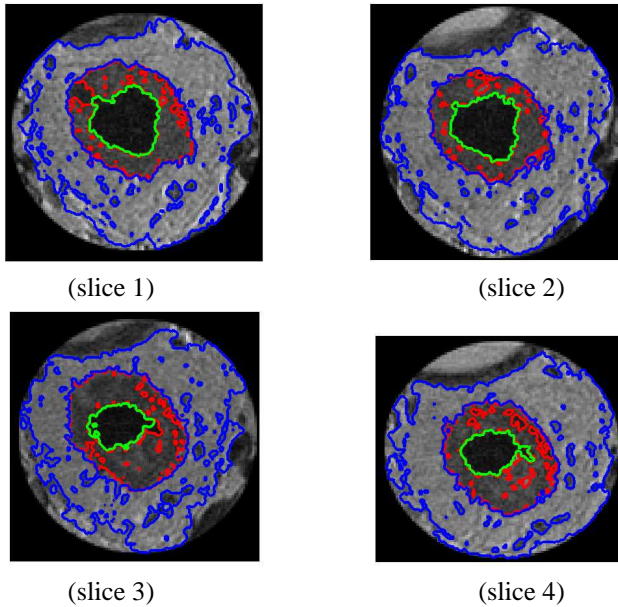


Fig. 1.7 Level set segmentation of four colorectal MR image slices using NPMM-ICLS algorithm. Colour code: green - colorectum, red - tumour, blue - mesorectum.

curvature based regularisation. At the same time there are certain regions which do not lie inside any of the zero level sets. This happens because the NPMM deems those regions to be partial volumed regions, and therefore the inhibition force stops the zero level sets entering into these regions. These regions can be further studied using more accurate pixel-by-pixel image analysis methods such as NPMM-ICLS algorithm. We also observe that there are small “holes” in the outermost segmentation class (mesorectum). Some of them are present in the consecutive slices whereas some of them disappear. Based on their pattern of appearance, one can either classify them as tubular(blood vessels) or ellipsoidal(lymph nodes) structures. This classification can potentially help deciding the stage to which colorectal cancer has grown. Not many reliable methods have been proposed so far to detect lymph nodes, and we believe our new method could be helpful for that task [Bond *et al.* (2007)].

Figure 1.8 shows various distributions involved in driving the level set solution. The NPMM-ICLS fitted PMF matches very closely with the overall intensity PMF, which shows better modelling of the intensity values. The individual class PMFs are also shown and have non-Gaussian shapes. To further verify the de-

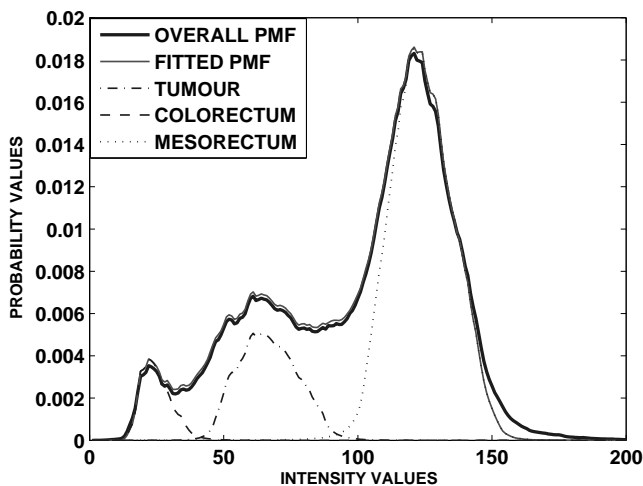


Fig. 1.8 Various distributions for the first slice of the colorectal MR images.

pendance of the segmentation procedure on Gaussian distribution assumption we performed the following experiment. We constrained the individual pure tissue class distributions to be Gaussian. The rest of the segmentation procedure was kept same. The results are shown in Fig. 1.9. Only the boundary of the mesorectum area (called as mesorectal fascia) is shown. The segmentation contour derived from GMM assumption drifts away from expected boundary location in the upper part of the image which is affected by the bias field. This clearly points out the need for modelling the intensity histogram with NPMM assumption.

Figure 1.10 shows a typical result for a natural image. Here we use only two pure classes namely, zebra and background, and no partial classes. The zero level set of the class “zebra” has also been shown. Figure 1.11 shows various PMFs involved in the experiment. Careful examination of the zebra image reveals that the class “zebra” has a bimodal PMF while the background has unimodal PMF. Although the zero level set of the zebra class segments it out quite satisfactorily, it is not a perfect segmentation. See, for example, the front leg and the region near its tail. This is because the characteristic striped texture is absent in these regions and the intensity values are very similar to that of the background. Therefore, the only distinguishing information is the edge between the two classes. Since we have not considered any edge or boundary information here, the zero level set is not “trapped” at the boundary of these two regions. The shapes of the individual

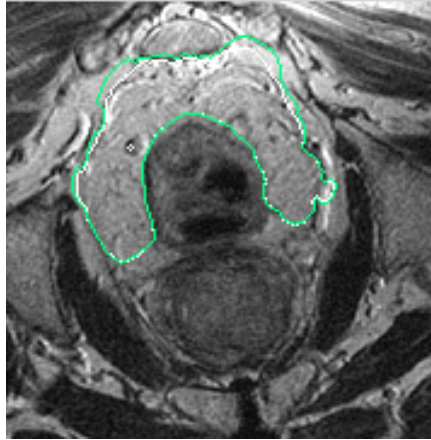


Fig. 1.9 Level set segmentation of mesorectal fascia using NPMM (white line) and GMM (green line). Level set contour evolved using GMM drifts away from expected boundary in the region affected by residual bias field.

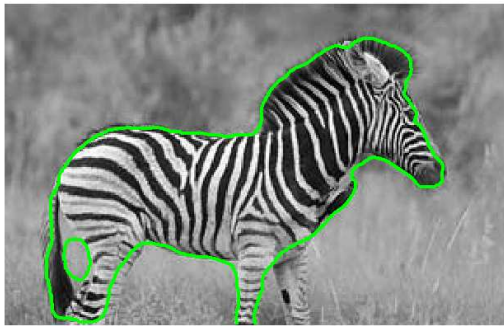


Fig. 1.10 Level set segmentation of zebra image with green coloured zero level set laid on the zebra class.

class PMFs demonstrate the non-Gaussian nature of the distributions involved and hence justify our use of the non-parametric estimation method of PMFs.

Finally, our method resembles the region competition method [Zhu and Yuille (1996)] and the method of Ref. [Paragios (2000)] in the sense that both these methods model the image histogram with mixture models. While they make use of Gaussian mixture models and likelihood probabilities, for the reasons stated earlier we use non-parametric distributions and their mixtures along with a *pos-*

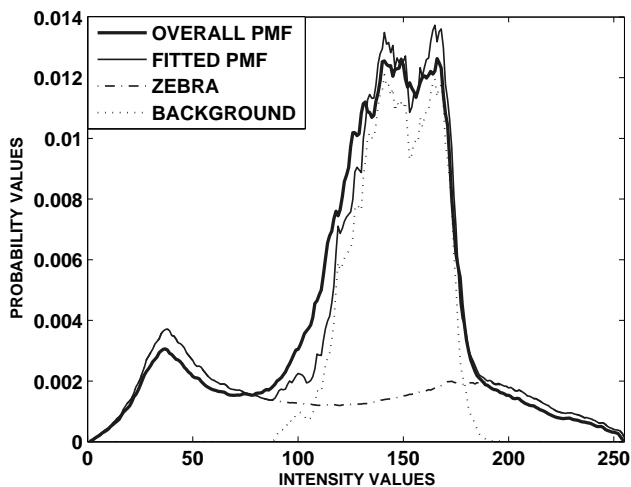


Fig. 1.11 Various distributions for the zebra image.

teriori probabilities. Also we take into account the partial volume effect which is particularly important in medical image analysis applications.

1.8 Conclusions

We presented a novel level set evolution method. The novelty of our algorithm stems out from the three contributions: non-parametric estimation of probability distributions using a recently proposed method, NPM-ICLS modelling of the image histogram, and accommodation of the partial volume effect. While the utility of each of the individual method has been shown already in various image analysis applications, we show here that they can be used for curve evolution purposes. A number of extensions to this method are in order. The most straightforward one is to work directly on 3D datasets. The colorectal MR datasets are acquired as a series of 2D images with a considerably lower resolution along the third dimension. Additional information along the third dimension is expected to improve the segmentation considerably, but the lower resolution along the third direction must be tackled. Another direction of improvement will be to incorporate the boundary information. Although the level set framework itself allows such incorporation very easily, set of features to be considered for the detection of

boundary seems to be a tricky issue. A quick look at Fig. 1.1 will show that the boundary of mesorectum is made up of variety of intensity changes such as step changes, ridges, and texture changes. Boundary information based on the magnitude of intensity gradients will be insufficient for such purposes as it only detects step changes in the intensity. And finally clinical validation of the segmentation procedure is needed. We have presented preliminary results on some of the issues mentioned above in our latest work [Bond *et al.* (2007)], the interested researchers are invited to read it.

Acknowledgement

This work is funded by EPSRC/MRC IRC MIAS, UK.

Bibliography

- Bond, S., Joshi, N. B., Petroudi, S. and Brady, M. (2007). Estimating the mesorectal fascia in mri, in *the proceedings of Information Processing in Medical Imaging - IPMI (to appear)*.
- Caselles, V., Kimmel, R. and Sapiro, G. (1997). Geodesic active contours, *International journal of computer vision* **22**, 1, pp. 61–79.
- Izenman, A. J. (1991). Recent developments in non-parametric density estimation, *Journal of the Americal Statistical Association* **86**, 413, pp. 205–224.
- Joshi, N. B. (2005). Non-parametric mixture model based segmentation of medical images, First year report, University of Oxford.
- Joshi, N. B. and Brady, M. (2005). A non-parametric mixture model for partial volume segmentation of MR images, in *the proceedings of British Machine Vision Conference - BMVC*.
- Kadir, T. and Brady, M. (2005). Non-parametric estimation of probability distributions from sampled signals, Tech. rep., OUEL No: 2283/05, (available at <http://www.robots.ox.ac.uk/~timork/PDFestimation/TR-2283-05.pdf>).
- Kim, J., Fisher, J. W., Yezzi, A., Cetin, M. and Willsky, A. S. (2005). A nonparametric statistical method for image segmentation using information theory and curve evolution, *IEEE trans. on image processing* **14**, 10, pp. 1486–1502.
- Leemput, K. V., Maes, F., Vandermuelen, D. and Suetens, P. (2003). A unifying framework for partial volume segmentation of brain MR images, *IEEE Trans. on Medical Imaging* **22**, 1, pp. 105–119.
- Papoulis, A. and Pillai, S. U. (2002). *Probability, random variables and stochastic processes* (McGraw-Hill).
- Paragios, N. (2000). *Geodesic active regions and level set methods: contributions and applications in artificial vision*, Ph.D. thesis, University of Nice Sophia Antipolis/INRIA, France.

- Sijbers, J. (1998). *Signal and noise estimation from magnetic resonance images*, Ph.D. thesis, University of Antwerp, Belgium.
- Sumengen, B. (). A matlab toolbox implementing level set methods, Tech. rep., Vision research lab, UC Santa Barbara, (available at http://barissumengen.com/level_set_methods/index.html).
- Zeydabadi, M., Zoroofi, R. A. and Soltanian-Zadeh, H. (2004). Multiresolution automatic segmentation of T1-weighted brain MR images, in *proceedings of IEEE international symposium on Biomedical imaging conference*, pp. 165–168.
- Zhu, S. C. and Yuille, A. (1996). Region competition: unifying snakes, region growing, and bayes/mdl for multiband image segmentation, *IEEE trans. on pattern analysis and machine intelligence* **18**, 9, pp. 884–900.